Xia, M., Ghafouri-Shiraz, H., Hou, L., and Kelly, A. E. (2017) High-speed pulse train amplification in semiconductor optical amplifiers with optimized bias current. *Applied Optics*, 56(4), pp. 1079-1086. (doi:10.1364/AO.56.001079)

High-speed Pulse Train Amplification in Semiconductor Optical Amplifiers with Optimized Bias Current

Mingjun Xia[1], H. Ghafouri-Shiraz[1], Lianping Hou,[2] and Anthony E. Kelly[2]

[1]*School of Engineering, University of Birmingham, Birmingham, B15 2TT, United Kingdom*

[2]*School of Engineering, University of Glasgow, Glasgow, G12 8LT, United Kingdom*

Received 27 Sept. 2016

In this paper we have experimentally investigated the optimized bias current of semiconductor optical amplifiers (SOAs) in order to achieve the high-speed input pulse train amplification with high gain and low distortion. Variations of the amplified output pulse duration with the amplifier bias currents have been analyzed and it is found that compared with the input pulse duration, the amplified output pulse duration is broadened; as the SOA bias current decreases from the high level (larger than the saturated bias current) to the low level, the broadened pulse duration of the amplified output pulse initially decreases slowly and then rapidly. Based on the analysis, an optimized bias current of SOA for high-speed pulse train amplification is introduced. The relations between the SOA optimized bias current and the parameters of the input pulse train (pulse duration, power and repetition rate) are experimentally studied. It is found that the larger input pulse duration, the lower input pulse power or the higher repetition rate can lead to a larger SOA optimized bias current, which corresponds to a larger optimized SOA gain. The effects of assist light injection and different amplifier temperatures on the SOA optimized bias current are studied and it is found that assist light injection can effectively increase the SOA optimized bias current while SOA has the lower optimized bias current at the temperature 20°C than that at other temperatures.

OCIS codes: *250.5980 (Semiconductor optical amplifiers), 250.5960 (Semiconductor lasers), (250.5530) Pulse propagation and temporal solitons*

1. INTRODUCTION

Semiconductor optical amplifiers (SOAs) have become the key devices in the integrated optical systems and passive optical networks (PON) for the advantages of high energy-efficient, wide operational bandwidth and small size [1-7]. However, the gain saturation mechanism in SOAs causes the distortion of the amplified output pulse. Injecting assist light [8], optimizing the structure of the active region [9-10] and doping the barrier region [11] were proposed to improve the gain dynamics of SOA while these measures can effectively accelerate the gain recovery rather than reduce the distortion of the amplified output pulse.

It is important to realize free-distortion amplification when SOA is adopted to amplify the optical synchronous clock signal or merge the multi-channel high-speed pulse trains [12-14]. For the generation of high repetition rate pulse trains, merging the pulse trains from the multiple channels each of which is amplified by SOA has become a promising method. However, the inconsistency in the amplified output pulse trains of the multiple channels, especially the difference in the pulse duration (full width at the half maximum) affects the performance of the high repetition rate pulse source. The pulse duration of the amplified output pulse depends on the amplifier's construction and operation conditions [15-17]. When the SOA bias current is high, optical pulse amplification suffers from distortion induced by the gain saturation. However, when the bias current is too low, the SOA gain also decreases [18-19]. Thus, it is significantly important to choose a suitable bias current for high-speed pulse train amplification in SOA. The pulse amplification in semiconductor optical amplifiers has been theoretical analyzed using the rate equations [20-21], the systematical analytical method [22] and the transmission line modelling method [6]. However, these theoretical analyses have made assumptions to obtain the analytic solutions or to aid the numerical computation, which has restricted the accuracy of the simulation results. In this paper, the detailed experiments are done to investigate the SOA optimized bias current for the high-speed pulse train amplification. As the SOA bias current decreases from the high level ($200mA$, more than the saturated level) to the low level ($30mA$), the pulse duration of the amplified output pulse is measured and analyzed. In order to realize high gain and low distortion amplification of the high-speed input pulse train, the SOA optimized bias current is defined based on the changes of the pulse duration of the amplified output pulse with the SOA bias currents. The relation between the SOA optimized bias current and the parameters of the SOA input pulse train (pulse duration, power as well as repetition rate) are experimentally studied. The effects of assist light injection and different temperatures on the SOA optimized bias current are analyzed.

This paper is organized as follows. The experimental system is introduced in Section 2. In Section 3, the optimized bias current for SOA is defined based on the variations of the pulse duration of the amplified output pulse with the SOA bias currents. In Section 4, the relation between the SOA optimized bias current and the input pulse duration, the input pulse power and the repetition rate of the pulse train is explored. In Section 5, the effects of assist light and temperature on the SOA optimized bias current is studied. Conclusions are given in section 6.

2. Experimental System

Figure 1(a) shows the schematic diagram of the experimental system for the high-speed pulse train amplification. The pulse train at the desired wavelength $1550nm$ is generated by the actively mode-locked fiber laser (MLFL), which is stimulated by the RF generator. The pulse train generated by the pulse laser is coupled to EDFA1 (Keopsys), which can provide the distortionless amplification for the pulse train. In order to obtain the pulse trains with different pulse durations from the PriTel pulse compressor, the power of the amplified output pulse train from EDFA1 can be adjusted by controlling the pump current of laser D1 in EDFA1. The optical attenuator is employed to control the power of the SOA input pulse train. The SOA input pulse train's repetition rate, power, pulse duration can be controlled by the pulse laser source, the optical attenuator and EDFA1, respectively. The optical spectrum analyzer (OSA), digital communication analyzer (DCA) and the RF analyzer are adopted to monitor the output of the pulse laser in the time-frequency domains. The SOA used in the experimental analysis is provided by the Compound Semiconductor Technologies Company. The bulk SOA is polarization-independent; the central wavelength of the SOA is $1554nm$ and its $3-dB$ bandwidth is $90nm$. The SOA temperature is set to be $20^{\circ}C$. In order to explore the SOA optimized bias current, the SOA bias current is decreased from $200mA$ (more than the saturated bias current) to $30mA$ and the step current is $5mA$. The SOA output pulse train is amplified by the free-distortion EDFA2 (PriTel) in order to ensure the measurement accuracy of the autocorrelator (Femtochrome). The corresponding physical map of the whole experimental system is shown in Fig. 1 (b).

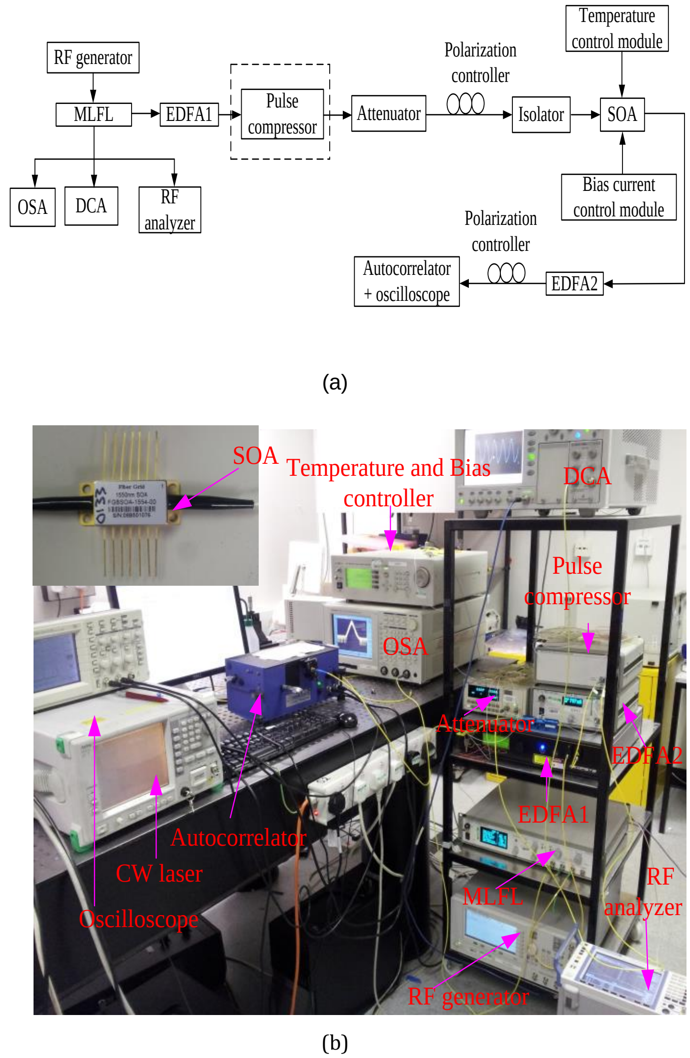

Fig. 1 Experimental system of SOA high-speed pulse train amplification (a) schematic diagram (b) physical map

3. Experimental Investigation of SOA Optimized Bias Current

In order to find experimentally the optimized value of the SOA bias current, we have measured variations of the pulse duration of the amplified output pulse train with SOA bias currents using the setup shown in Fig. 1 (b). The input of EDFA1 as shown in Fig. 1(a), is a $10GHz$ pulse train at the wavelength $1550nm$ which is generated by MLFL and its amplified output pulse train duration and power can be changed by the pulse compressor and optical attenuator, respectively. This output is then injected into the SOA input. The function of distortionless EDFA2 is to increase the output power of the SOA which can effectively improve the accuracy of the autocorrelation measurement. Fig. 2 shows the measured amplified output pulse autocorrelation results. As the results show there are two pulses in the autocorrelator response during the fixed $320ps$ measurement time interval. It should be noted that number of the pulses per a given fixed time interval is determined by the repetition rate of the pulse train. It is found that the pulse train generated by pulse laser (see Fig.1(a)) can be closely approximated to the Gaussian pulse, which has a better fitting result as compared with other pulse shapes. Thus, based on the autocorrelation response we can find the best Gaussian fitted response from which we can obtain the pulse duration of each pulse in the train. We have found that by dividing the duration of each pulse in the auto-correlation response by $\sqrt{2}$ the actual pulse duration can be obtained.

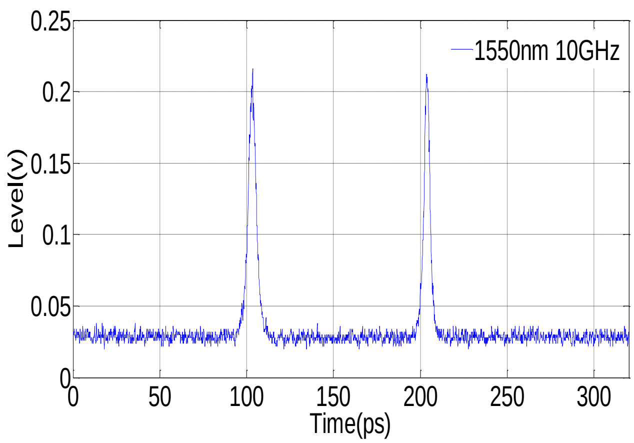

Fig. 2 Schematic diagram of the pulse duration measurement using the autocorrelator

Prior to the exploration experiments, SOA characteristic curves are measured. Fig. 3 shows the variations of the forward (blue curve) and backward (green curve) ASE output powers and the corresponding amplifier active region voltage (red curve) with respect to the SOA bias currents without applying any external optical signal at its input. It is found that as the SOA bias current increases from $30mA$ to $200mA$, the forward and backward output power first increases rapidly and then slowly due to the SOA gain saturation. Results in Fig.3 show that the difference between the forward and backward output power at different bias current is very small, which indicates that the SOA is in a good operating condition. The voltage value of the amplifier active region is measured by the bias current control module (i.e. Temperature and bias controllers in Fig. 1(b)).

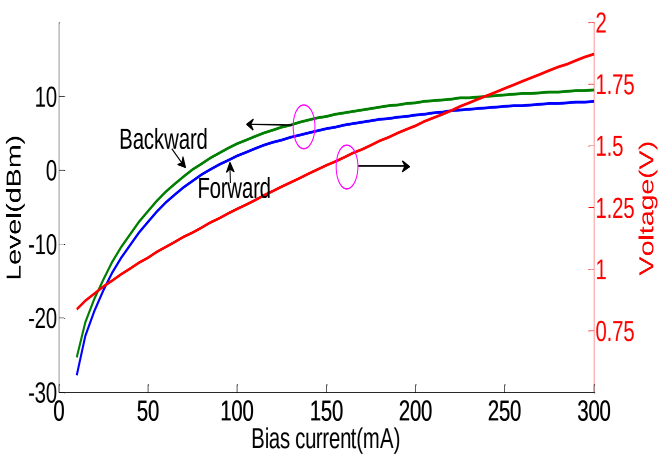

Fig. 3 SOA characteristic curves ASE output power vs bias current (blue and green curves)and voltage of the amplifier active region vs bias current (red curve)

Figure 4 shows the variations of the pulse duration of the amplified output pulse and the corresponding SOA gain with different SOA bias currents when the pulse duration of the SOA input pulse train is $1.37ps$. The pulse train centered at the wavelength $1550nm$ with a repetition rate $10GHz$ is generated by the pulse laser.

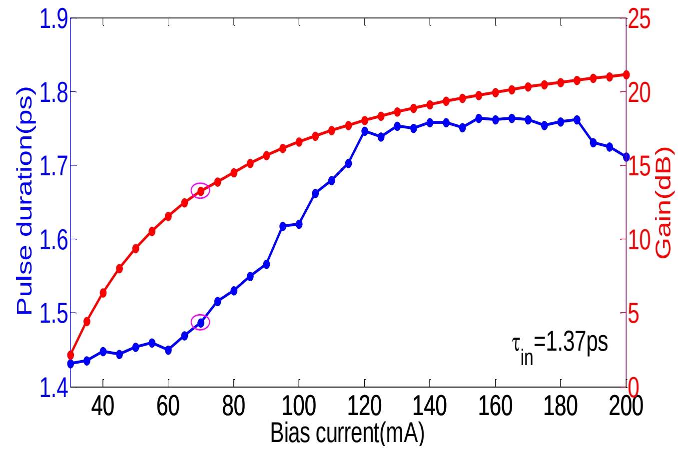

Fig. 4 Variations of the pulse duration of amplified output pulse train (blue curve) and the SOA gain (red curve) with the different bias currents at the input pulse duration $1.37ps$.

From the blue curve in Fig. 4, it can be observed that as the SOA bias current I decreases from $200mA$ to $30mA$, the pulse duration of the SOA amplified output pulse first decreases very slowly ($120mA \le I \le 200mA$) and then decrease quickly ($30mA \le I < 120mA$). The minimum pulse duration of the amplified output pulse is $1.43ps$, which indicates that the pulse duration of the amplified output pulse is larger than that of the input pulse at all the bias currents ranging from $200mA$ to $30mA$. From the red curve in Fig. 4, it is found that as the bias current decreases from $200mA$ to $30mA$, the SOA gain decreases from $21.14dB$ to $2.17dB$. Here, the SOA gain is obtained by measuring the difference between the peak of the SOA input pulse spectrum and the peak of the SOA output pulse spectrum.

The above analysis shows that when the optical pulse train is amplified by the SOA at a high bias current, the pulse duration of the amplified output pulse is broadened due to the enhancement of the spontaneous emission and carrier heating effects. In order to reduce the pulse duration broadening, the SOA bias current can be decreased from the high level to the low level. However, the low bias current restricts the amplification ability of SOAs. Thus, choosing a suitable bias current is important to realize the SOA pulse train amplification with low distortion and high gain. In the following, the SOA optimized bias current is defined. The SOA bias current I is decreased from the level higher than the saturated bias current to the low level until the pulse duration of the amplified output pulse satisfies the relation equation

$$\tau_{out} \le \beta \tau_{in} \quad (1)$$

where, τ_{out} is the duration of the amplified output pulse, β is the coefficient for the SOA bias current optimization, τ_{in} is the duration of the SOA input pulse. Then, the optimized bias current I_m can be defined as

$$I_m = \max(I),\ where,\ I\ satisfies\ \tau_{out} \le \beta\tau_{in} \qquad \textbf{(2)}$$

In the following experimental analysis, the SOA bias current optimization coefficient β is set to be 1.1. In the above example τ_{in} is $1.37ps$ and $\beta\tau_{in}\ (\beta = 1.1)$ is $1.507ps$. Based on Eqs.(1-2), the SOA optimized bias current is $70mA$ and the corresponding optimized gain is $13.25dB$, which have been marked in Fig. 4.

4. Relation between SOA Optimized Bias Current and Input Pulse Duration, Power, Repetition Rate

The above analysis has shown that how to choose an optimized bias current for the pulse train amplification with less pulse duration broadening and high gain. In this section, experimental analyses are done to study the relation between the optimized bias current and the parameters of the input pulse train (pulse duration, power and repetition rate).

4.1 Relation between SOA Optimized Bias Current and Input Pulse Duration

In order to explore the relation between the SOA optimized bias current and the input pulse duration, the pulse duration of the $10GHz$ pulse train at the wavelength $1550nm$ are tuned by changing the EDFA1 pump current. Fig. 5 shows the relation curve between the pulse duration of the SOA input pulse and the EDFA1 pump current. It is found that as the EDFA1 pump current increases from $700mA$ to $1100mA$, the SOA input pulse duration varies from $4.95ps$ to $1.37ps$. As the compressed pulse trains with different pulse durations have different powers, an optical attenuator is adopted to fix the power of the SOA input pulse train at $-18.4dBm$.

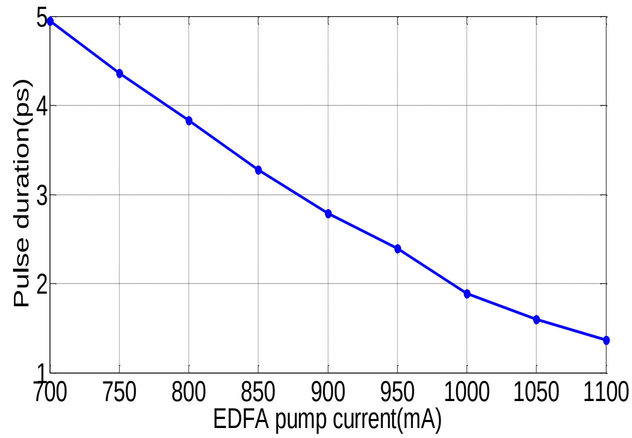

Fig. 5 Pulse duration of SOA input pulse train vs EDFA1 pump currents

Figure 6 shows the variations of the pulse duration of amplified output pulse train with the SOA bias currents at the different input pulse durations. For each EDFA1 pump current, as the SOA bias current reduces, the variation process of the pulse duration of the amplified output pulses can be divided into the slow decrease stage and the fast decrease stage. It is found that as the pulse duration of the input pulse increases from $1.60ps$ to $2.79ps$ (i.e. the EDFA1 pump current decreases from $1050mA$ to $900mA$), the threshold bias current between the two stages increases from $130mA$ to $155mA$ and the variation range of the pulse duration of the SOA amplified output pulse ($30mA \le I \le 200mA$, I is the SOA bias current) decreases from $0.647ps$ to $0.404ps$, which indicates that the pulse train with the narrower pulse duration is more easily broadened in the SOA amplification process. The corresponding SOA optimized bias current has been labelled in Fig. 6.

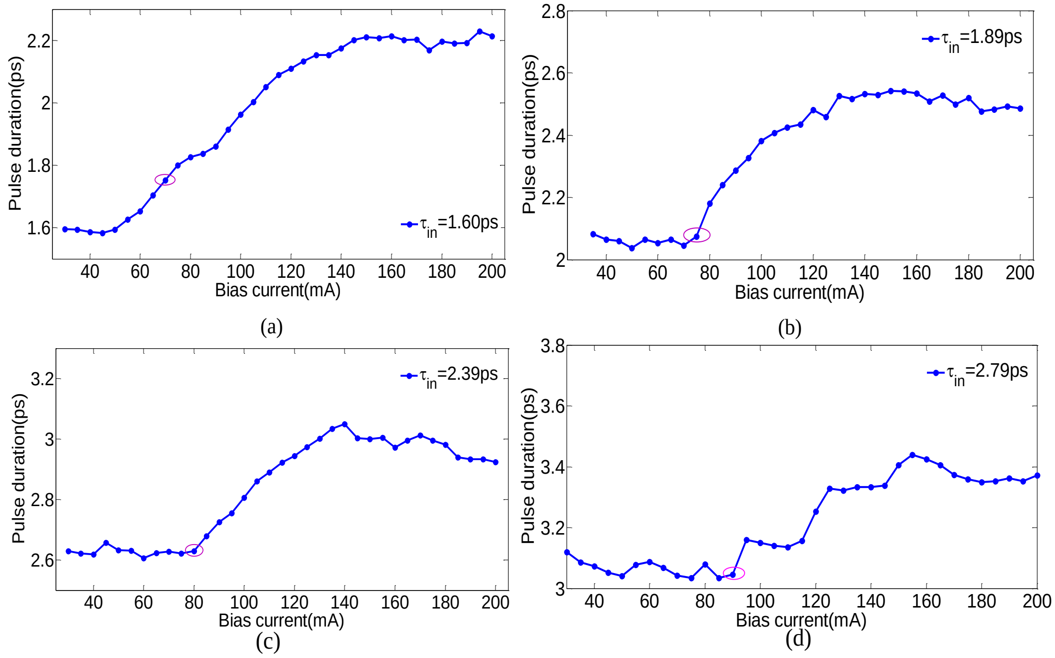

Fig. 6 Pulse duration of amplified output pulse train vs SOA bias currents at different input pulse durations (a) 1.60ps (b) 1.89ps (c) 2.39ps (d) 2.79ps

Figure 7 (a) shows the schematic diagram of the input pulse train with different pulse durations at the same input power. Fig. 7 (b) shows the variations of the SOA optimized bias currents at the different input pulse durations (blue line) and the SOA gain at the corresponding optimized bias current (red line). It is found that as the input pulse duration increases, the SOA optimized bias current increases and the SOA gain at the corresponding optimized bias also increases, which indicates that for the same input power, the pulse train with the larger pulse duration can be amplified without distortion at a higher gain.

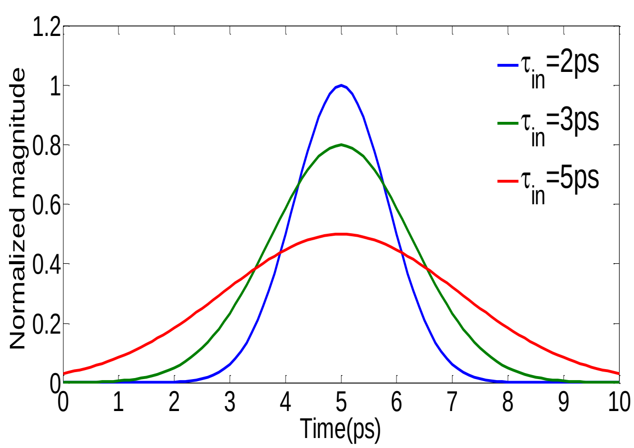

(a)

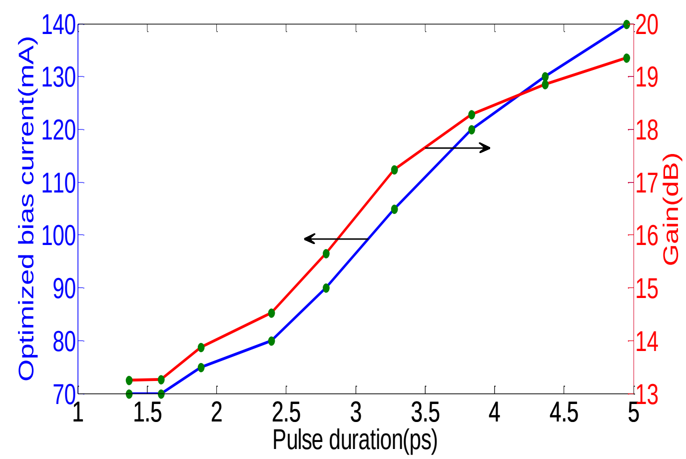

(b)

Fig. 7 (a) Schematic diagram of the input pulse train with different pulse durations (b) variations of the SOA optimized bias currents and the SOA optimized gain at the different input pulse durations

4.2 Relation between SOA Optimized Bias Current and Input Pulse Power

The power of the SOA input pulse train is an important parameter that influences the gain dynamics. In the following, the relation between the SOA optimized bias current and the power of the input pulse train is studied. The pulse compressor is removed from the experimental system. The pulse train with the central wavelength 1550nm at the repetition rate 10GHz is generated by MLFL. The power of the SOA input pulse train is adjusted by the optical attenuator. The above analysis has shown that the pulse duration can influence the SOA optimized bias current and thus the first step is to explore whether the duration of the SOA input pulse train will be changed in the process of attenuation. Fig. 8 shows the pulse duration of the SOA input pulse train at the different attenuation values. It is found that as the attenuation values of the optical attenuator increases from $0dB$ to $10dB$, there is almost no variation of the pulse duration of the SOA input pulse train. The maximum value of the pulse duration is $3.247ps$ while the minimum value is $3.118ps$. Based on Fig. 7 (b), the small pulse duration variation ($0.129ps$) has little influence on the SOA optimized bias current. Fig. 8 can confirm that the effects of the pulse duration variation of the SOA input pulse train induced by the optical attenuator on the SOA optimized bias current is negligible.

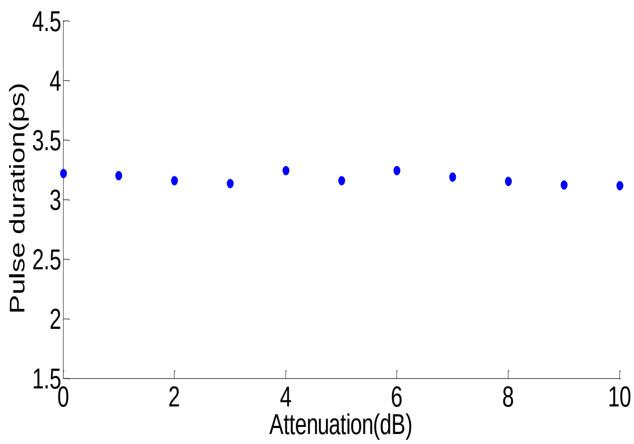

Fig. 8 Variation of the pulse duration of the SOA input pulse train at the different optical attenuation values

Figure 9 shows the variation of the SOA optimized bias current at the different attenuation values (blue line) and the SOA gain at the corresponding SOA optimized bias current (red line). It is found that as the value of the attenuator increases, which means that the power of the SOA input pulse train decreases, the optimized bias current increases and meanwhile the optimized SOA gain increases. This can be explained that when the power of the input pulse train is high, the amplification of the pulse leading edge depletes more carriers, which leads to lower carrier density level in the amplifier cavity; then the gain for the amplification of the pulse tailing edge is smaller. The inconsistent amplification between the leading edge and the tailing edge of the same pulse induces larger distortion of the amplified output pulse. Thus in this case that the input pulse train has a higher power, the optimized bias current and the optimized SOA gain are lower.

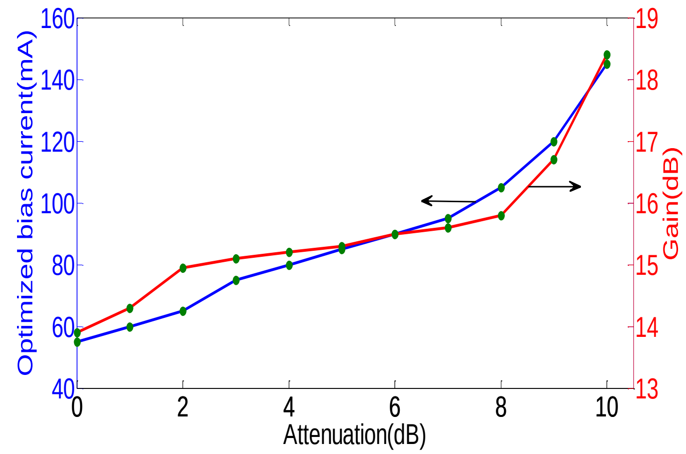

Fig. 9 Variations of SOA optimized bias currents and SOA optimized gain at the different attenuation values

4.3 Relation between SOA Optimized Bias Current and the Repetition Rate of the Input Pulse Train

Figure 10 shows the variations of the SOA optimized bias current at the different repetition rates of the input pulse train and the SOA gain at the corresponding optimized bias currents. The power and the pulse duration of the SOA input pulse train are $-14dBm$ and $3.2ps$, respectively. It is found that the SOA optimized bias current becomes larger at a higher repetition rate. This is because when the repetition rate of the input pulse train is high, the time interval between two adjacent pulses is short, which means there is less time for carrier density recovery and thus the carrier density level in the SOA cavity is lower. In this case that the input pulse train with a high repetition rate is amplified, SOA are more difficult to be saturated, which indicates that it is allowed to provide a larger SOA bias current to accelerate the carrier density recovery (shown in Fig. 11).

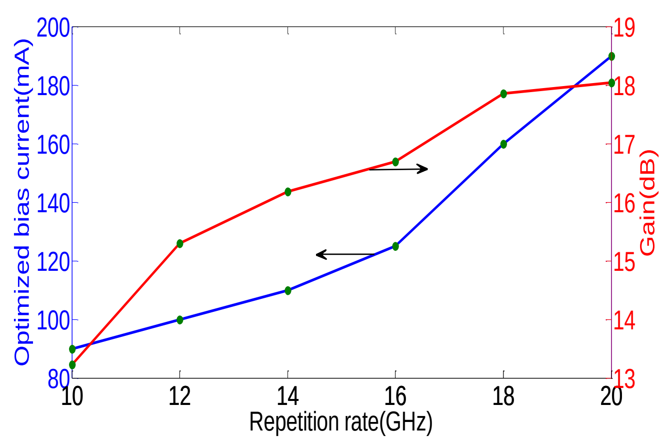

Fig. 10 Variations of the SOA optimized bias currents and SOA optimized gain at the different repetition rates of pulse trains

The pump-probe experiments are done to analyze the relation between the SOA bias current and the SOA carrier density recovery speed. The wavelengths for the pump and probe signal are $1550nm$ and $1555nm$, respectively. The forward pump signal is the pulse train with the input power $10dBm$ and FWHM (full width at half maximum) $3.2ps$ at the repetition rate $10GHz$ and the backward continuous probe signal has the magnitude $0dBm$. Fig. 11 shows the temporal output waveform of the amplified CW probe signal at the different SOA bias currents ($100mA$, $120mA$ and $150mA$) measured by DCA. It is found that as the SOA bias current increases, the average output power in a pulse period ($100ps$) is higher, which indicates a faster carrier density recovery resulting in a higher carrier density level in the amplifier cavity. The experimental results further confirm the accuracy of the analysis of the relation between the SOA optimized bias current and the repetition rate of the pulse train.

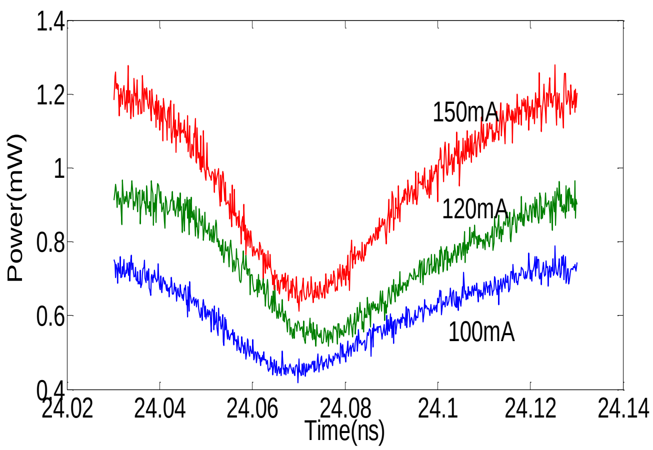

Fig. 11 Temporal output waveform of the amplified CW probe signal at the different SOA bias currents

5. Effects of Assist Light Injection and Temperature on SOA Optimized Bias Current

5.1 Effects of Assist Light Injection on the SOA Optimized Bias Current

Gain region light injection can reduce the spectral broadening, and shifting of the SOA amplified output pulse while it also decreases the carrier density level in the amplifier cavity [8]. In this section, the effects of gain region light injection on the SOA optimized bias current at the different repetition rates of the input pulse train are studied. The continuous wave (CW) assist light at the wavelength $1535nm$ with the magnitude $2dBm$ is counter-propagated into the SOA through the optical circulator and the pulse train at the wavelength $1550nm$ is forward injected into the SOA. The small signal gain for the CW assist light is 7.5dB, which indicates that the power level of the injected gain region assist light almost saturates the SOA due to the fact that the SOA saturation output power is around 10dBm (shown in Fig. 3).

The schematic diagram for the experimental system is shown in Fig. 12. Fig. 13 shows the variations of SOA optimized bias currents at the different repetition rates with and without assist light. It is found that the assist light injection enlarged the SOA optimized bias current. This is because the amplification of injected assist light takes part in depleting the carrier density and thus there exists a lower carrier density level in the amplifier cavity, which means that SOA suffer from the gain saturation at a higher SOA bias current injection. Also, it is found that as the repetition rate of the input pulse train increases, the difference between the optimized bias current with assist light injection and that without assist light injection becomes smaller. This can be explained that at a higher repetition rate for the input pulse train, there exists a lower carrier density in the amplifier cavity due to the smaller recovery time between the adjacent pulses of the pulse train, which leads to a smaller decrease of carrier density with the amplification of the gain region assist light.

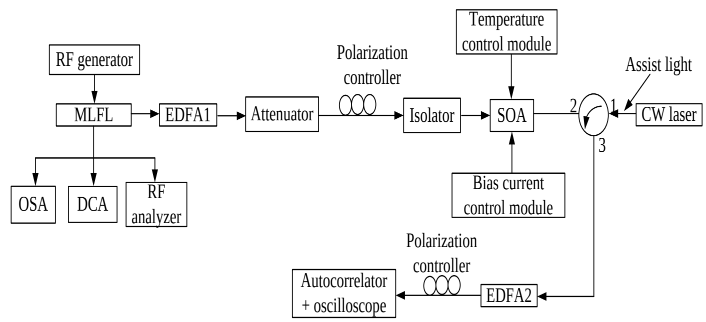

Fig. 12 Schematic diagram of the experimental system for high-speed pulse train amplification with the assist light injection

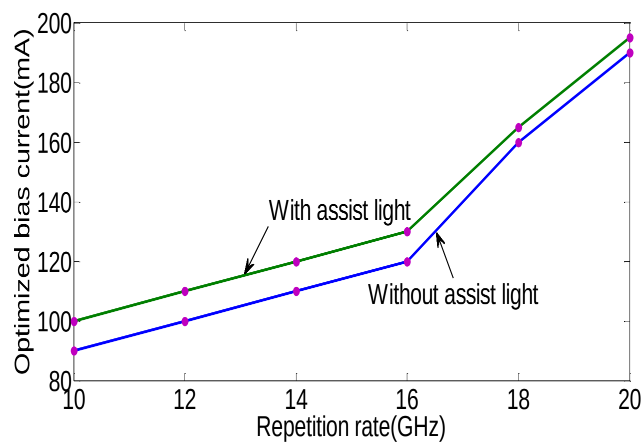

Fig. 13 Variations of the SOA optimized bias currents at the different pulse train repetition rates with and without assist light

5.2 Relation between the SOA temperature and the SOA optimized bias current

The SOA temperature has an important influence on its dynamic gain [4, 23]. In this section, the relation between the SOA operation temperature (T) and the optimized bias current is explored. Figure 14 shows the experimental results. It is found that as the SOA temperature increases from $5^{\circ}C$ to $40^{\circ}C$ the SOA optimized bias current first decreases and then increases; at the temperature $20^{\circ}C$ the optimized bias current arrive at the minimum value $75mA$. This is because the SOA gain value at the input pulse's wavelength

$1550nm$ at working temperature $20^{\circ}C$ are larger than those at other temperatures, which can be found in the temperature-dependent SOA gain (shown in Fig. 15). From Fig. 15, It is found that as the SOA temperature increases, the peak of the SOA gain shifts to the longer wavelength and the gain value decreases. This is because as the operation temperature increases, the Quasi Fermi-level in the SOA conduction band becomes lower while the Quasi Fermi-level in the SOA valence band becomes higher. This determines that the SOA at the operation temperature $20^{\circ}C$ can be saturated at a lower bias current.

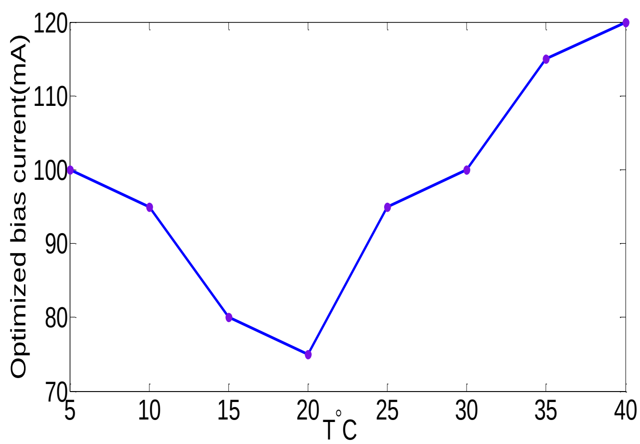

Fig. 14 Variations of SOA optimized bias currents at the different temperatures

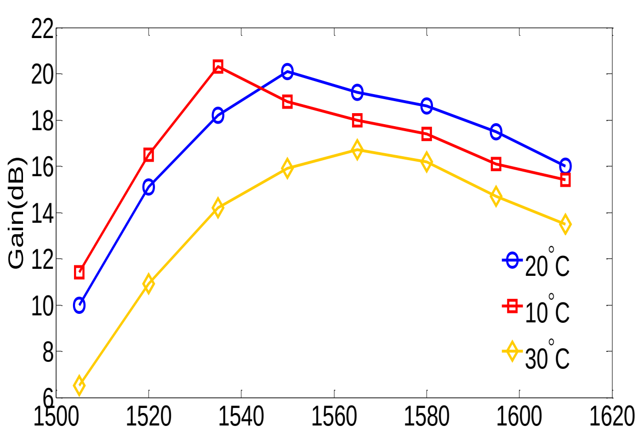

Fig. 15 SOA gain at the different wavelengths with different operation temperatures

6 Conclusions

In this paper, experimental studies are done to show how the bias current of a SOA can be optimized so that high gain and very low distortion amplification can be achieved when a high-speed optical pulse train enters the amplifier input. We have explored the variations of the amplified pulse duration with the amplifier bias current and based on this investigation the amplifier optimized bias current for high gain and low distortion pulse amplification is defined. Experiments are done to investigate the relationships between the amplifier optimized bias current and input pulse train duration, power and repetition rate. Also, effects of the amplifier working temperature and assist light injection on the amplifier optimized bias current are studied.These experimental results provide an effective guidance to choose suitable bias currents to realize low-distortion and high-gain pulse train amplification in the practical application of SOAs.

REFERENCES

[1] A.R. Totovic, J.V.Crnjanski, M.M. Krstic, M.L.Masanovic, and D.M. Gvozdic, "A self-consistent numerical method for calculation of steady-state characteristics of traveling-wave and reflective SOAs," IEEE Journal of Selected Topics in Quantum Electronics, **19**, Art. No. 3000411, (2013).

[2] S. Nakamura, Y. Ueno, and K. Tajima, "Femtosecond switching with semiconductor-optical-amplifier-based Symmetric Mach-Zehnder-type all-optical switch," Applied Physics Letters, **78**, 3929-3931 (2001).

[3] A. Capua, O. Karni, G. Eisenstein, V. Sichkovskyi, V. Ivanov, and J. P. Reithmaier, "Coherent control in a semiconductor optical amplifier operating at room temperature," Nature Commun., **5**, Art. ID 5025 (2014).

[4] M. Xia and H. Ghafouri-Shiraz, "Analysis of carrier heating effects in quantum well semiconductor optical amplifiers considering holes' non-parabolic density of states," Optical Quantum Electronics, **47**, 1847-1858 (2015).

[5] S. Chandrasekhar, Xiang. Liu, Peter. J. Winzer, J. E. Simsarian, and R. A. Griffin, "Compact all-InP laser-vector-modulator for generation and transmission of 100-Gb/s PDM-QPSK and 200-Gb/s PDM-16-QAM," IEEE J. Lightw. Technol., **32**, 736-742 (2014).

[6] M. Xia and H. Ghafouri-Shiraz, "Wavelength-dependent femtosecond pulse amplification in wide band tapered-waveguide quantum well semiconductor optical amplifiers," Applied Optics, **54**, 10524-10531 (2015).

[7] J. Akbar, O. A. Odedina, C. Michie, I. Andonovic and A. E. Kelly, "Monolithic adjustable gain-clamped semiconductor optical amplifier", IEEE J. Lightwave Technol., **31**, 2723-2727 (2013).

[8] H. Wang, J. Wu, and J.T. Lin, "Spectral characteristics of optical pulse amplification in SOA under assist light injection", J. Lightwave Technol. **23**, 2761–2771 (2005).

[9] A. V. Uskov, J. Mørk, B. Tromborg, T. W. Berg, I. Magnusdottir, and E. P. O'Reilly, "On high-speed cross-gain modulation without pattern effects in quantum dot semiconductor optical amplifiers," Opt. Commun.,**227**, 363–369 (2003).

[10] V. V. Lysak, H. Kawaguchi, I. A. Sukhoivanov, T. Katayama, and A. V. Shulika, "Ultrafast gain dynamics in asymmetrical multiple quantumwell semiconductor optical amplifiers," IEEE J. Quantum Electron., **41**, 797–807(2005).

[11] L. Zhang, I. Kang, A. Bhardwaj, N. Sauer, S. Cabot, J. Jaques, and D. T. Neilson, "Reduced recovery time semiconductor optical amplifier using p-type-doped multiple quantum wells," IEEE Photon. Technol. Lett., **18**, 2323–2325 (2006).

[12] M. Zhu, N. Cvijetic, M. F. Huang, T. Wang, and G. K. Chang, "Low-Latency synchronous clock distribution and recovery for DWDM-OFDMA-based optical mobile backhaul," IEEE J. Lightwave Technol., **32**, 2012-2018 (2014).

[13] J. B. Khurgin, I. Vurgraftman, J. R. Meyer, S. Xu and J. U. Kang, "Reduced crosstalk semiconductor optical amplifiers based on Type-II quantum wells," IEEE Photon. Technol. Lett., **14**, 278-280 (2002).

[14] T. Nakahara and R. Takahashi, "Self-stabilizing optical clock pulse-train generator using SOA and saturable absorber for asynchronous optical packet processing," Optics Express,**21**, 10712 (2013).

[15] M. Kolarczik1, N. Owschimikow, J. Korn, B. Lingnau, E. Schol, Y. Kaptan, D. Bimberg, K. Ludge and U. Woggon, "Quantum coherence induces pulse shape modification in a semiconductor optical amplifier at room temperature," Nature Commun., **4**: 2953, (2013).

[16] M. Matsuura, H. Ohta and R. Seki, "Experimental investigation of chirp properties induced by signal amplification in quantum-dot semiconductor optical amplifiers," Opt. Lett. **40**, 914-917 (2015).

[17] K.Hussain and P. K. Datta, "Effect of including intraband phenomena in the semiconductor optical amplifier model for propagation of short pulses," Applied Optics, **52**, 7171-7177 (2013).

[18] S. Porto, C Antony, P. Ossieur and P. D. Townsend, "An upstream reach-extender for 10Gb/s PON applications based on an optimized semiconductor amplifier cascade," Optics Express, **20**, 186-191 (2011).

[19]G. Talli and M. J. Adams, "Gain dynamics of semiconductor optical amplifiers and three-wavelength devices," IEEE Journal of Quantum Electronics, **39**, 1305-1312 (2003).

[20] L. M. Frantz and J. S. Nodvik, "Theory of pulse propagation in a laser amplifier," J. Appl. Phys., **34**, 2346–2349 (1963).

[21] M. Xia and H. Ghafouri-Shiraz, "Optimization of Pump current for pulse distortionless amplification in quantum well amplifiers," IEEE J. Lightwave Technol., **33**, 3907-3913 (2015).

[22] M. Premaratne, D. Nesic, and G. P. Agrawal, "Pulse amplification and gain recovery in semiconductor optical amplifiers: a systematic analytical approach," IEEE J. Lightwave Technol., **26**, 1653-1660 (2008).

[23] Y. Jiao et al. "Measurement and analysis of temperature dependent optical model gain in single-layer InAs/InP(100) quantum dot amplifiers in the 1.6 μm to $1.8 \mu m$ range", IEEE J Photonics, **4**, 2292-2306 (2012).